Sound and Light from Fractures in Scintillators

A. Tantot,[1,2] S. Santucci,[3] O. Ramos,[2] S. Deschanel,[4,1] M.-A. Verdier,[1] E. Mony,[1]
Y. Wei,[1] S. Ciliberto,[3] L. Vanel,[2] and P. C. F. Di Stefano[1,*]

[1]*Department of Physics, Queen's University, Kingston, Ontario K7L 3N6, Canada*
[2]*Institut Lumière Matière, UMR5306 Université de Lyon 1-CNRS, Université de Lyon, F-69622 Villeurbanne Cedex, France*
[3]*Université de Lyon, Laboratoire de Physique, École Normale Supérieure de Lyon,
Centre National de la Recherche Scientifique UMR 5672, 46 Allée d'Italie, F-69364 Lyon Cedex 07, France*
[4]*MATEIS, UMR 5510 CNRS and INSA-Lyon, Université de Lyon, F-69621 Villeurbanne, France*
(Received 16 May 2013; published 10 October 2013)

Prompted by intriguing events observed in certain particle-physics searches for rare events, we study light and acoustic emission simultaneously in some inorganic scintillators subject to mechanical stress. We observe mechanoluminescence in $Bi_4Ge_3O_{12}$, $CdWO_4$, and $ZnWO_4$, in various mechanical configurations at room temperature and ambient pressure. We analyze the temporal and amplitude correlations between the light emission and the acoustic emission during fracture. A novel application of the precise energy calibration of $Bi_4Ge_3O_{12}$ provided by radioactive sources allows us to deduce that the fraction of elastic energy converted to light is at least 3×10^{-5}.

Rare-event searches in particle physics, like those looking for particle dark matter [1], employ draconian measures to reduce all forms of background that could hide their signal. The main background is usually of radioactive nature; however, other forms are possible. For instance, the first, calorimetric phase of the CRESST experiment measured phonons in sapphire crystals cooled to around 10 mK to detect particle interactions [2]. Initially, thermal contraction of the holders caused fractures in the crystals, limiting sensitivity of the experiment by 3 orders of magnitude in rate above the radioactive background until the problem was identified [3,4]. Certain more recent experiments use a coupled measurement of phonons and scintillation to determine the nature of the interacting particles and reject the radioactive background [5]. However, mechanoluminescence, i.e., the emission of light by a solid subject to mechanical stress, occurs in many materials [6], including plastic scintillators [7]. In addition, correlated acoustic emission (AE) and visible-photon emission have been observed during mechanical deformation of colored alkali halides [8]. Other types of emission, including electrons [9], positive ions [10], and x rays [11], have also been studied in various materials under mechanical stress. Nevertheless, there is an opinion that fracture events in scintillation-phonon detectors would produce little or no light (e.g., Ref. [12]).

Prompted by recent intriguing events observed by the CRESST II dark matter search using cryogenic scintillation-phonon $CaWO_4$ detectors [5], we study mechanoluminescence as a form of photon-producing background in such devices. We also argue that photon emission can help characterize the rupture dynamics in a manner analogous to AE [13–15] and can provide complementary information about the fracture energy. To investigate these two points, we have carried out what we believe are the first experiments to correlate the acoustic and light emission from common scintillators under mechanical stress and to quantify the conversion of elastic energy into light.

Our studies involve the measurement of acoustic phonons and luminescence as a piece of scintillating crystal is stressed to the point of rupture. The inorganic scintillators studied here are widely used in particle detection [16,17]: bismuth germanate ($Bi_4Ge_3O_{12}$, also known as BGO), zinc tungstate ($ZnWO_4$), and cadmium tungstate ($CdWO_4$). Except where specified, all samples were kindly supplied by Crystal Manufacturing Lab, Ltd., Novosibirsk. We have tested two loading geometries, at room temperature and ambient pressure. Initially, $20 \times 10 \times 5$ mm^3 rectangular prisms were indented by a steel bead driven by a manual screw, causing the material to break in multiple fragments. In order to better control the rupture process, we subsequently adopted the double cleavage drilled compression (DCDC) geometry [18] (Fig. 1). These samples were
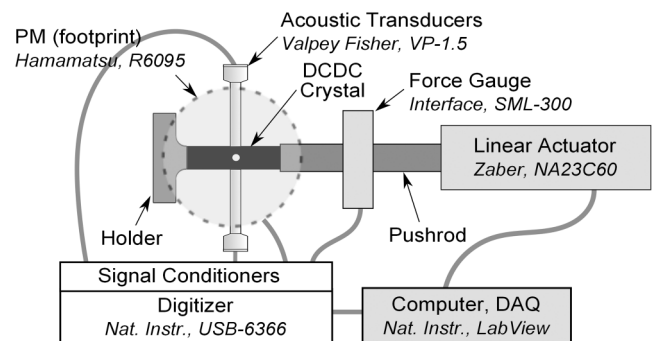

FIG. 1. Actuator-driven experimental setup with DCDC sample geometry.

$20 \times 5 \times 3$ mm^3 rectangular prisms, polished to optical quality, with a 1 mm diameter circular hole drilled perpendicularly in the middle of the 20×5 mm^2 face. Under compression along the long axis, cracks formed reproducibly on either side of the hole in the plane parallel to the 20×3 mm^2 face. Unlike BGO, tungstates have a cleavage plane [19]; orientation of the crystals was chosen so that this plane was parallel to the DCDC fracture direction. The DCDC samples were pressed against a backstop by a push rod that was driven by an actuator (controlled manually in early experiments and by computer in later ones). This geometry provides some control of crack velocity via the applied compressive stress, up to a critical length, at which point the sample cleaves abruptly [18]. A force gauge in the push rod measured the load imposed by displacements of the actuator. The acoustic activity was recorded by two piezoelectric transducers in contact with opposite sides of the crystal via ultrasound gel. Light emission was recorded by a standard bialkali photomultiplier (PM) covering the crystal. The output of the PM was integrated with a time constant ranging from 1.8 to 10 μs, depending on the sample, to produce a signal that could be digitized more slowly than the raw PM output. All four channels (force, 2 AE, PM) were digitized at a rate of 2×10^6 samples per second in a continuous stream. The set point of the computer-controlled actuator was also recorded.

The fracture procedure involves advancing the actuator by small steps (down to 0.1 μm). Each step is followed by a waiting time of at least 30 s. The whole procedure lasts 1–2 h, during which we continuously monitor AE and PM activity. Figure 2 shows typical observations for the
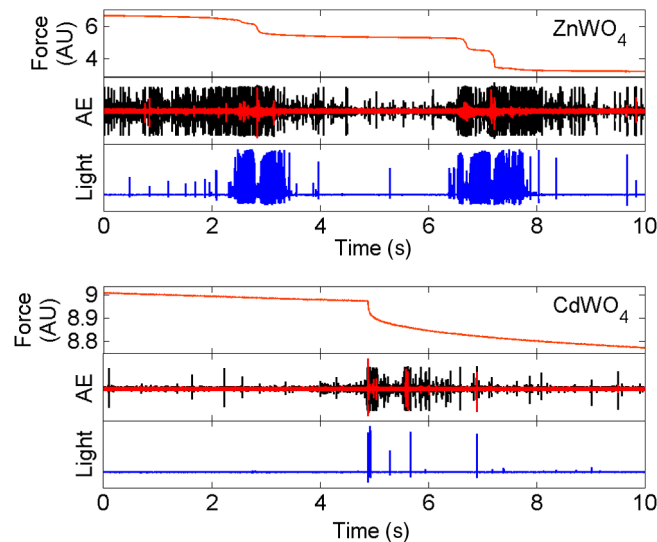
tungstate crystals. Spurts of activity on the AE and PM channels are correlated to drops in the force. These abrupt force relaxations are a direct consequence of crack growth in the samples. There is also a regime in which the force decreases slowly and during which other processes, such as rearrangements and dislocations, produce AE and PM signals [8]. Similar correlations have been observed for other materials, such as colored KBr [8], composites [20], and silica glass [21].

Indentation of BGO samples (from Fibercryst, France) also produces correlated AE and light signals. These correlations can be analyzed more quantitatively by looking at the statistical properties of individual acoustic and light events. In this analysis, individual events have been determined on each channel by requiring that the signal surpass a threshold and that it be separated from the previous event by at least a minimum time. Figure 3 shows that the distributions of waiting times between events are similar for AE and light over two decades. For light events, it is possible to obtain a much smaller minimum separation time (1.5 μs) than for AE (250 μs), since the former pulses are shorter than the latter.

To quantify the amount of light emitted and to investigate the emission mechanism, we next compared the spectra of light emitted by BGO (sample from Fibercryst) during fracture and during scintillation stimulated by x rays. To avoid afterglow from the high dose of x rays, the fracture spectrum was measured first, and then one of the fragments was measured while being irradiated by x rays. The measurements of the light spectra were carried out with a monochromator and a CCD camera. In the x-ray excitation configuration, a generator provided x rays with a broad spectrum up to a few tens of keV. Over the recorded range of wavelengths, both resulting spectra (Fig. 4) show a very similar shape (as is the case for many materials [22]), indicating a common underlying luminescence mechanism, at least for the last stages of light emission. The likeness of our spectra to previous work on BGO indicates this last stage involves $^3P_1 \rightarrow {}^1S_0$

FIG. 2 (color online). 10 s samples from observations of manually compressed DCDC specimens of CdWO$_4$ and ZnWO$_4$. In each figure, top to bottom: applied force, both AE signals, and light signal. Drops in the force indicating fracture are correlated to increased acoustic and photon activity. All signals are uncalibrated.
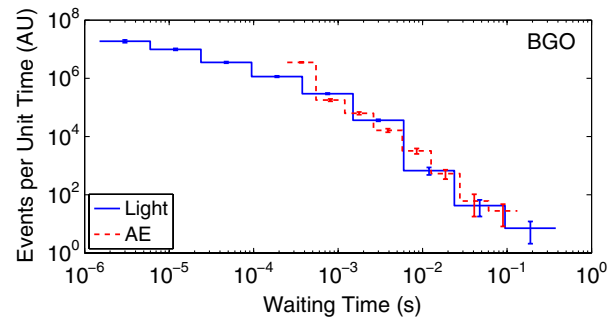

FIG. 3 (color online). Waiting times between light events and between AE events during the indentation of a BGO sample. Both channels show similar behavior over the shared part of the range, with the shorter light pulses providing better timing separation than the longer AE ones.
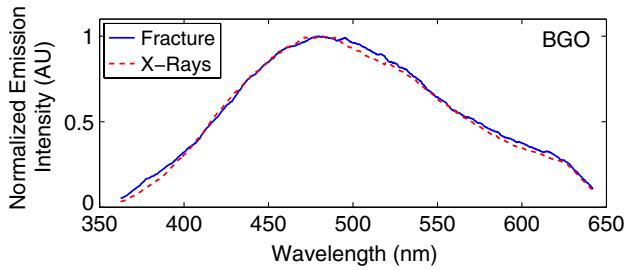
FIG. 4 (color online).   Emission spectra from a BGO sample,
first during fracture, then under x-ray excitation. The similarity
of spectra indicates a common emission mechanism.

electronic transitions of the Bi^{3+} luminescence centers
[23]. This measurement does not determine if the fractures
excite the luminescence centers directly. It cannot be
excluded that the crystal is indirectly excited by particles
produced by fractoemission [9] interacting in the scintilla-
tor. For instance, if x rays or electrons are produced, the
BGO sample would be quite efficient at detecting them
itself (attenuation length ≈ 20 μm for 10 keV x rays [24]),
as opposed to needing an external x-ray detector [11].
Alternatively, any UV light (potentially from arcs in the
atmosphere near the fracture) might be reabsorbed in
the scintillator since BGO absorbs wavelengths below
≈ 300 nm [25].

We then calibrated the light channel for a DCDC BGO
sample using radioactive γ-ray sources as we would cali-
brate a regular scintillator used for particle detection.
Calibration was carried out in the main DCDC setup and
with the standard data acquisition system (Fig. 1). The
analysis involves extracting individual events as described
earlier and then building the distribution of the event
integrals. The integral of an event, like its amplitude, is a

proxy for the energy deposited by the γ ray, so we can
identify the peaks in the distribution corresponding to the
energies of the radioactive sources and of backscattering
[16], as shown in Fig. 5. Over the energy range available
with these sources, the crystal and readout behave in a
linear manner with respect to the energy deposited in the
scintillator, and we extrapolate this calibration to higher
energies. Calibrations before and after the fracture are
compatible to within 10%. From the standpoint of the
scintillation mechanism, γ rays and x rays can interact in
inorganic scintillators via the photoelectric effect or
through Compton scattering, creating a primary electron-
hole pair which eventually transfers a portion of the depos-
ited energy to the luminescence centers (Bi^{3+} for BGO).
For a given light signal, calibrations provide the equivalent
amount of energy deposited by a γ ray. This can be con-
verted to the actual energy of the emitted light by knowing
the light yield of the scintillator (8 photons/keV for γ rays
in BGO [16]) and the energy of individual scintillation
photons (2.6 eV; cf. Fig. 4).

The calibrated BGO crystal was then fractured in the
main DCDC setup, using the protocol described earlier. We
focus on the last drop in force, occurring when the crack
splits the sample in two. Figure 6 shows that the overall
behavior is similar to that observed for the tungstates. The
photon channel displays a wide distribution of event ampli-
tudes. They in fact reach up to the saturation level of
the integrator, equivalent to γ-ray energy deposits of
≈ 85 MeV—a testimony to the amount of light emitted.
There is also a hint of increased photonic activity before
the main fracture occurs. The correlations are better quan-
tified in Fig. 7, illustrating the cumulative number of events
on the acoustic channels and those on the photon channel.
Minimum separation time required between photon events
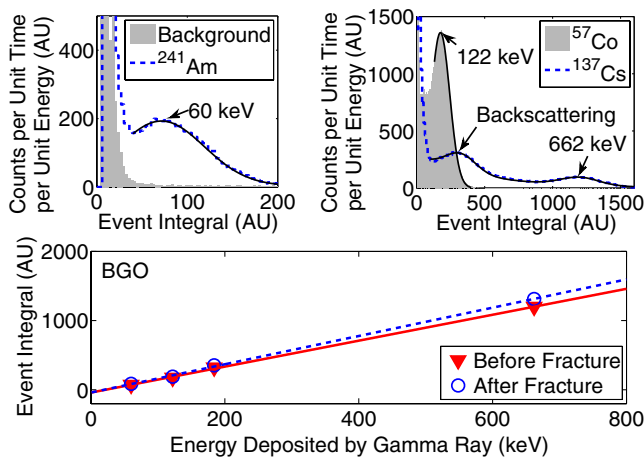was 10 μs, and 1 ms between AE events. On all three

FIG. 5 (color online).   Energy calibration of a DCDC BGO
scintillator using radioactive sources. Top: Spectra for various
sources and fits to the full-collection and backscattering peaks.
Bottom: Response of the system is fairly linear over this energy
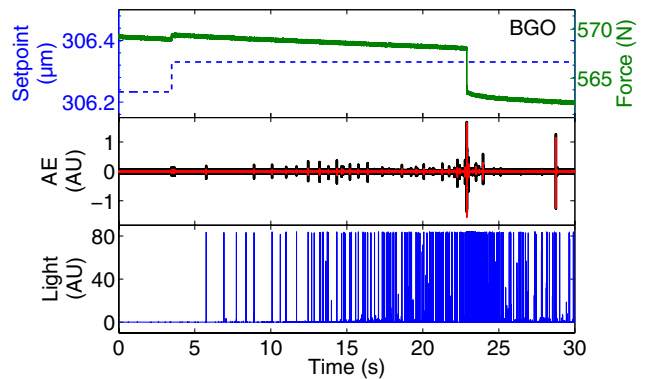range and varies by $\approx 10\%$ after the fracture.

FIG. 6 (color online).   Zoom on the rupture of the DCDC BGO
sample of Fig. 5 showing correlation between the various chan-
nels when the main fracture occurs around 23 s (corresponding
to ≈ 17 min since the start of the procedure). Photon signal
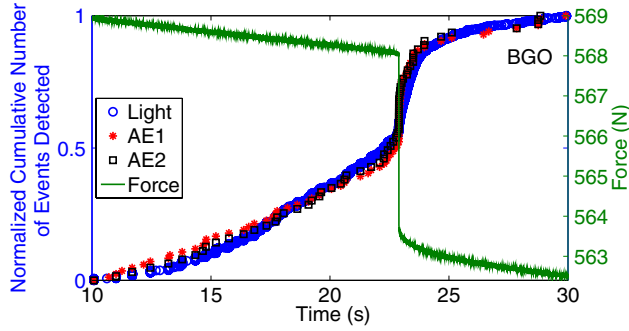shows a wide range of amplitudes (the largest of which saturate
the integrator).

FIG. 7 (color online).   Normalized cumulative number of events on AE and photon channels around the main fracture, for the BGO sample of Fig. 6. The AE and photon channels show similar behavior. The drop in force signaling the main fracture corresponds to a sharp increase in the event rates for photons and AE.

channels, the cumulative number of events rises steadily with a slight increase in slope until the fracture, as determined by the drop in the force. This drop marks a sharp increase in the slope of cumulative events that eventually peters out. When normalized to the total number of events on each channel, all curves are very similar. Last, event amplitudes for all channels are power-law distributed (Fig. 8). For both AE channels, the exponents are -1.7 ± 0.2 (errors are one standard deviation). Assuming the AE energy is proportional to the amplitude squared, the power-law distribution of the energy would have as an exponent -1.4 ± 0.1. This is compatible with the exponent obtained for the light channel -1.2 ± 0.2, for which amplitude is proportional to energy. A more precise measurement might check if the absolute value of the AE exponent is in fact larger than that of the light channel, an indication of dissipation in the acoustic channel [26].

We can also use our technique to estimate certain contributions to the energy budget of the rupture process in BGO. Elastic energy is converted into broken bonds, phonons (that are either measured as acoustic emission or decay into heat), and light. For the emitted light, the calibrations with γ-ray sources establish that the total amount of emitted light is equivalent to that caused by
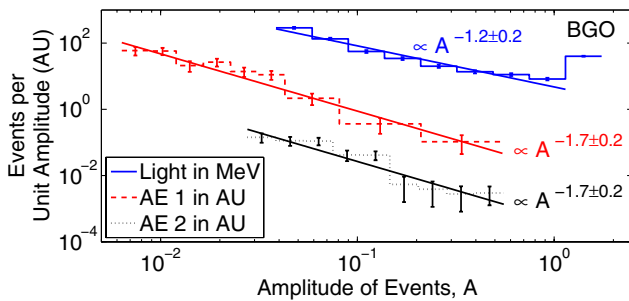

FIG. 8 (color online).   Amplitude distributions for the various channels of the BGO sample from Fig. 6. Amplitude of the light channel is proportional to energy. All distributions are fitted by power laws (up to saturation, for light).

γ-ray energy deposits of at least 300 GeV, in other words, a total energy converted to light greater than 6.2 GeV. Only a lower bound is set because of the integrator saturation mentioned previously. Eighty-five percent of this light is emitted in a 20 s window centered on the main fracture. We next estimate the drop in elastic energy of the crystal during the main fracture. Neglecting the hole in the DCDC geometry, the elastic energy in the crystal of section S (perpendicular to the force F) and of volume V is $(F/S)^2 \times (V/2E)$, where E is Young's modulus. Applying a standard acoustic measurement of longitudinal and shear waves [27] to BGO, we find $E = 139 \pm 4$ GPa, somewhat above the range of published values (up to 106 ± 10 GPa [28] and references therein). Assuming the loaded volume and surface vary little, the drop in force of ≈ 5 N is equivalent to a drop in elastic energy of ≈ 30 μJ. Since the surface created during the fracture is roughly $20 \times 3 = 60$ mm^2, this amounts to a surface creation energy of the order of 1 J/m^2, consistent with the scales typically found for crystals (e.g., 0.28 J/m^2 for BaF$_2$ and 1.2 J/m^2 for MgO [29]). Furthermore, the conversion efficiency of elastic to luminous energy is therefore at least 6.5 GeV/30 μJ $\approx 3 \times 10^{-5}$. A fuller understanding of the energy budget requires knowledge of the energy transformed into phonons, or heat. The standard room-temperature technique to study brittle fracture only involves measurement of acoustic phonons using acoustic emission. We are not aware of any work quantifying the fraction of energy going into acoustic phonons or calibrating the energy scale of acoustic phonons. The harder-to-implement technique of cryogenic calorimetry would allow measurement of all the phonons and would therefore provide more insight into the energy budget [30].

We have evidenced correlated mechanical-stress-induced emission of photons and of phonons in several common inorganic scintillators used for particle detection (Bi$_4$Ge$_3$O$_{12}$, ZnWO$_4$, and CdWO$_4$), at room temperature and in a normal atmosphere. At least for BGO, both emissions share similar distributions of waiting times over several decades. Also for BGO, the two energy distributions are similar, and the wavelength of fractoluminescence is the same as that of scintillation. In a mechanically stressed scintillation-only detector, the power-law distribution of mechanoluminescence energies means that spurious low-energy events may mimic dark matter ones. It seems reasonable to assume our results apply to other tungstates, and it would be interesting to study the light-phonon correlations of individual fracture events in CRESST II–like conditions of vacuum and low temperature (other background-based explanations of the intriguing CRESST II events have been proposed [31]). In addition, the reabsorption of products of fractoemission could affect other types of solid-state particle detectors (e.g., ionization or ionization-phonon ones [1,16]). From the standpoint of fracture physics, in contrast to previous

studies by acoustic emission or by spectrally resolved luminescence (e.g. Ref. [32]), our use of the light channel offers a precisely calibrated energy scale. This allows us to quantify the amount of elastic energy converted into light and is a step toward a better fundamental understanding of fracture mechanisms.

---

*Corresponding author.
distefan@queensu.ca

[1] R. W. Schnee, in *Physics of the Large and Small: Proceedings of the 2009 Theoretical Advanced Study Institute in Elementary Particle Physics*, edited by C. Csaki and S. Dodelson (World Scientific, Singapore, 2010), p. 629.

[2] G. Angloher *et al.* (CRESST Collaboration), Astropart. Phys. **18**, 43 (2002).

[3] J. Astrom *et al.*, Phys. Lett. A **356**, 262 (2006).

[4] P. Di Stefano *et al.* (CRESST Collaboration), AIP Conf. Proc. **555**, 381 (2001).

[5] G. Angloher *et al.* (CRESST II Collaboration), Eur. Phys. J. C **72**, 1 (2012).

[6] J. I. Zink, Naturwissenschaften **68**, 507 (1981).

[7] G. Reynolds and R. Austin, J. Lumin. **92**, 79 (2000).

[8] B. P. Chandra, J. Phys. D **17**, 117 (1984).

[9] S. C. Langford, J. T. Dickinson, and L. C. Jensen, J. Appl. Phys. **62**, 1437 (1987).

[10] J. T. Dickinson, A. Jahan-Latibari, and L. C. Jensen, J. Mater. Sci. **20**, 229 (1985).

[11] C. G. Camara, J. V. Escobar, J. R. Hird, and S. J. Putterman, Nature (London) **455**, 1089 (2008).

[12] R. J. Gaitskell, in *Proceedings of the Third International Workshop on the Identification of Dark Matter*, edited by N. J. Spooner and V. Kudryatsev (World Scientific, Singapore, 2000), p. 606.

[13] K. Mogi, Bull. Earthquake Res. Inst. **40**, 125 (1962).

[14] A. Garcimartin, A. Guarino, L. Bellon, and S. Ciliberto, Phys. Rev. Lett. **79**, 3202 (1997).

[15] S. Deschanel, L. Vanel, G. Vigier, N. Godin, and S. Ciliberto, Int. J. Fract. **140**, 87 (2006).

[16] G. F. Knoll, *Radiation Detection and Measurement* (Wiley, New York, 2000), 3rd ed.

[17] P. A. Rodnyi, *Physical Processes in Inorganic Scintillators* (CRC Press, Boca Raton, FL, 1997), 1st ed.

[18] Special issue on the 10th International Congress on Glass [C. Janssen, J. Ceram. Soc. Jpn. **10**, 23 (1974)].

[19] F. Danevich, V. Kobychev, S. Nagorny, D. Poda, V. Tretyak, S. Yurchenko, and Y. Zdesenko, Nucl. Instrum. Methods Phys. Res., Sect. A **544**, 553 (2005).

[20] A. Crasto, R. Corey, J. Dickinson, R. Subramanian, and Y. Eckstein, Compos. Sci. Technol. **30**, 35 (1987).

[21] Y. Kawaguchi, Phys. Rev. B **52**, 9224 (1995).

[22] J. Duignan, I. Oswald, I. Sage, L. Sweeting, K. Tanaka, T. Ishihara, K. Hirao, and G. Bourhill, J. Lumin. **97**, 115 (2002).

[23] M. J. Weber and R. R. Monchamp, J. Appl. Phys. **44**, 5495 (1973).

[24] B. Henke, E. Gullikson, and J. Davis, At. Data Nucl. Data Tables **54**, 181 (1993).

[25] F. Rogemond, C. Pedrini, B. Moine, and G. Boulon, J. Lumin. **33**, 455 (1985).

[26] Z. Olami, H. J. S. Feder, and K. Christensen, Phys. Rev. Lett. **68**, 1244 (1992).

[27] J. Krautkrämer and H. Krautkrämer, *Ultrasonic Testing of Materials* (Springer, New York, 1990), 4th ed.

[28] M. Lebeau, J. Mater. Sci. Lett. **4**, 779 (1985).

[29] J. J. Gilman, J. Appl. Phys. **31**, 2208 (1960).

[30] J. Astrom, P. Di Stefano, F. Proebst, L. Stodolsky, and J. Timonen, arXiv:0708.4315.

[31] M. Kuźniak, M. Boulay, and T. Pollmann, Astropart. Phys. **36**, 77 (2012).

[32] G. Pallares, C. L. Rountree, L. Douillard, F. Charra, and E. Bouchaud, Europhys. Lett. **99**, 28 003 (2012).